Electronic Supplementary Information

Effective Ensemble System for Identification of CN^-, Based on Cobalt (II) Complex: Mimicking Logic Gate†

Nirma Maurya, Ashok Kumar Singh

Department of Chemistry, Indian Institute of Technology-Roorkee,
Roorkee-247667, India
*E-mail: akscyfcy@iitr.ernet.in

ESI Fig. S1: Interaction of 2a with 10 eq. of metal ions (a) absorption spectra (b) emission spectra in H_2O-DMF (1:9, v/v, HEPES buffer 7.4).

ESI Fig. S2: Benesi-Hilderbrand Plot for the binding constant of **2a** towards $\mathbf{Co^{2+}}$ **(**a) absorbance (b) emission spectra.

ESI Fig. S3: Effect of pH (a) and water content (b) on emission intensity of **2a+**$\mathbf{Co^{2+}}$ complex.

ESI Fig. S4: Benesi-Hilderbrand Plot for the binding constant of **2a+** $\mathbf{Co^{2+}}$ complex towards $\mathbf{CN^-}$ absorbance spectra **(**a) (0-1.4) eq. CN^- (b) (1.4-3.0) eq. CN^- and (c) emission spectra.

ESI Fig. S5: (a) Calibration curve for **2a+**$\mathbf{Co^{2+}}$ **complex** and (b) calibration sensitivity for $\mathbf{CN^-}$ ion in H_2O-DMF (1:9, v/v, HEPES buffer 7.4).

ESI Fig. S6: IR spectra of (a) **2a+**$\mathbf{Co^{2+}}$ complex and (b) **2a +**$\mathbf{Co^{2+}}$**+**$\mathbf{CN^-}$ complex.

ESI Fig. S7: Mass spectrum of **2a+**$\mathbf{Co^{2+}}$ complex.

ESI Fig. S8: Mass spectrum of **2a +**$\mathbf{Co^{2+}}$**+**$\mathbf{CN^-}$ adduct.

ESI Fig. S9: FTIR spectrum of **2a**.

ESI Fig. S10: ^{1}H NMR spectrum of **2a** in DMSO- d_6.

ESI Fig. S11: ^{13}C spectrum of **2a** in $CDCl_3$

ESI Fig. S12: Mass spectrum of **2a.**

ESI Fig. S13: ^{1}H NMR spectrum of **2b** in $CDCl_3$

ESI Fig. S14: ^{13}C spectrum of **2b** in $CDCl_3$.

ESI Fig. S15: ^{1}H NMR spectrum of **1** in $CDCl_3$.

ESI Fig. S16: ^{13}C spectrum of **1** in $CDCl_3$.

ESI Fig. S17: (a) Absorption titration spectra (b) Emission titration spectra of 2b upon addition of Co^{2+} in H_2O-DMF (1:9, v/v, HEPES buffer 7.4).

Table S1: Recovery analysis of spiked CN^- concentration in deionized water, river water and tap water samples[a].

Experimental Section

Chemical and Instrumentation

All reagents and solvents for experimental work were taken from Sigma–Aldrich. DMF solvent was dried with the help of $CaCl_2$ as drying agent and then stored on molecular sieve after distillation process (under reduced pressure). CHNS (carbon, hydrogen, nitrogen, sulfur) elemental analysis was supported by using a vireo MICROV3.1.1. IR spectra were recorded with Perkin Elmer FT-IR 1000 spectrophotometer (KBr solid film). Specord S600 Thermo-Scientific PC double beam spectrophotometer used for absorption spectra with quartz cuvette of path length 1 cm. Horiba RF-5301PC was used for emission spectra with standard quartz cell of path length 3 cm. The NMR spectra were recorded in JEOL 400 MHz spectrophotometer by applying tetramethylsilane (TMS) as an internal standard. The cyclic voltammograms were note down with a CHI760E Electro analyzer three-electrode cell with glassy carbon as the working electrode, $Hg/HgCl_2$ as the reference electrode, Pt wire as the counter electrode and 0.1 M tetrabutylammonium perchlorate (TBAP) was used as the supporting electrolyte on 0.1V s^{-1} scan rate.

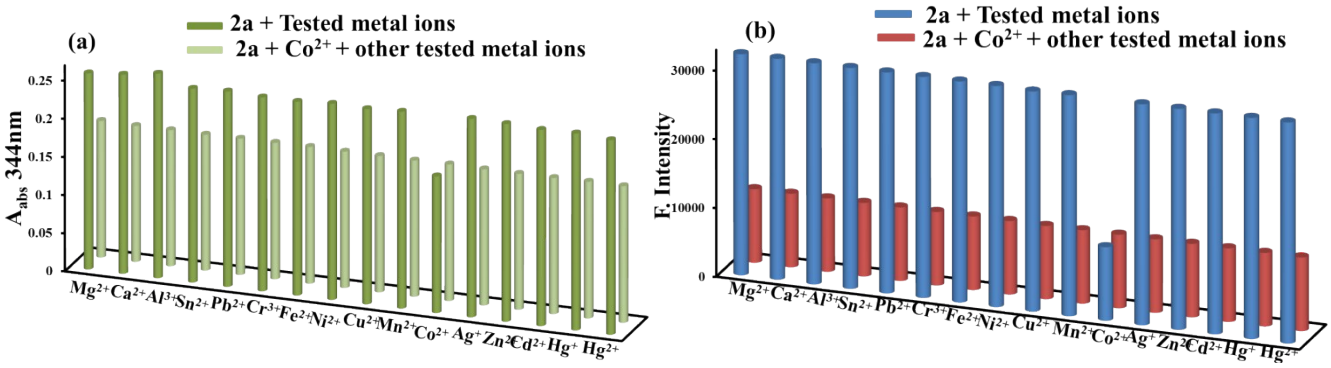

ESI Fig. S1: Interaction of 2a with 10 eq. of metal ions (a) absorption spectra (b) emission spectra in H_2O-DMF (1:9, v/v, HEPES buffer 7.4).

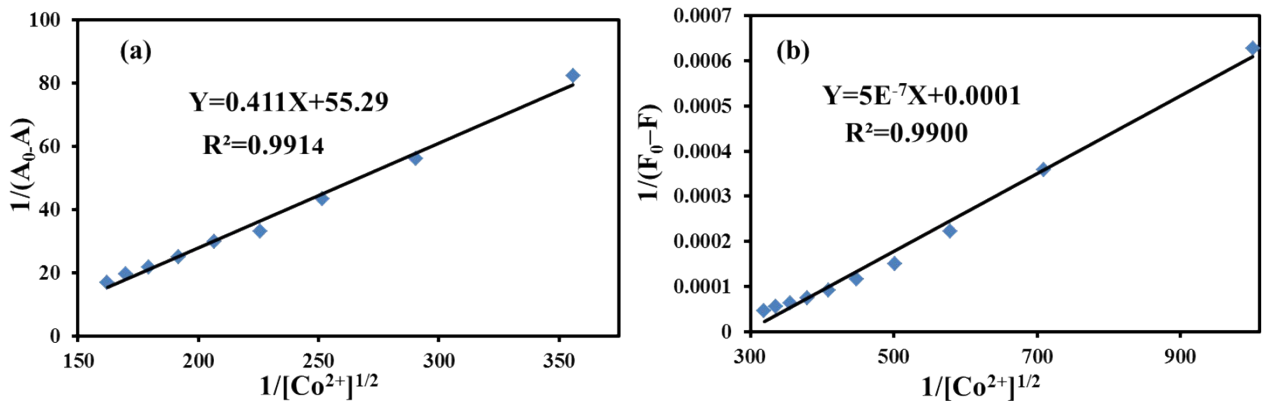

ESI Fig. S2: Benesi-Hilderbrand Plot for the binding constant of **2a** towards **Co^{2+}** (a) absorbance (b) emission spectra.

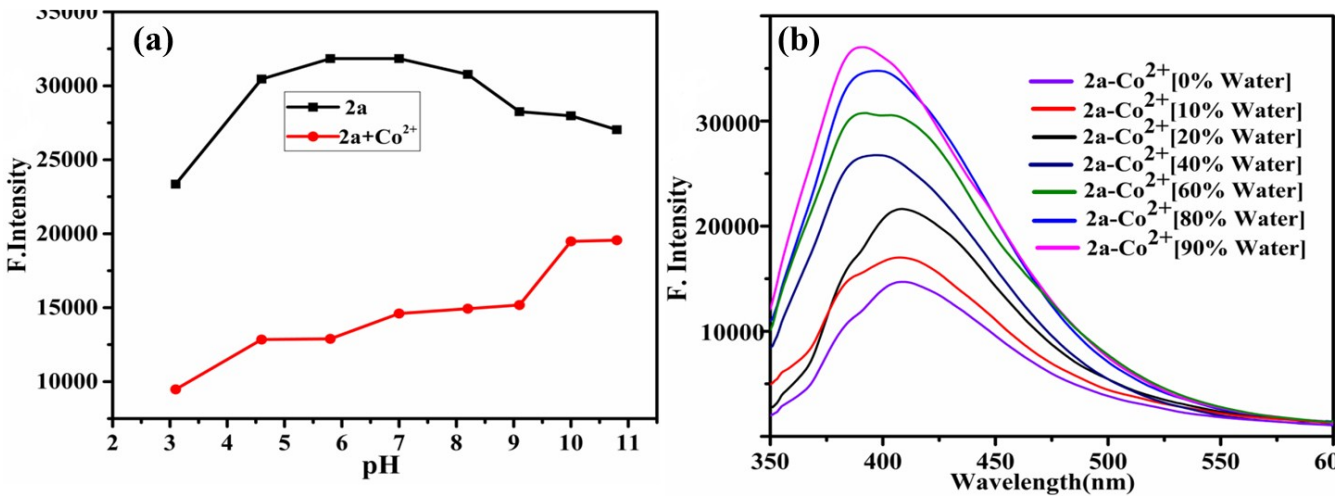

ESI Fig. 3 Effect of pH (a) and water content (b) on emission intensity of **2a+Co^{2+}** complex.

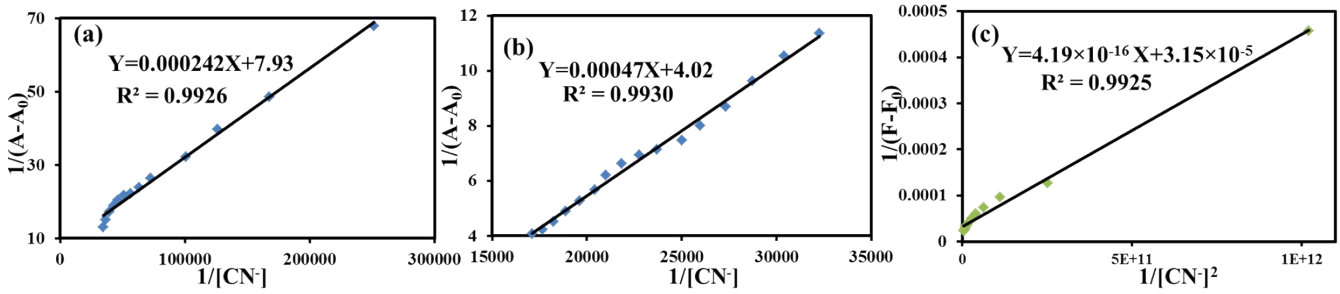

ESI Fig. S4: Benesi-Hilderbrand Plot for the binding constant of **2a+ Co^{2+}** complex towards **CN^{-}** absorbance spectra **(**a) (0-1.4) eq. CN^{-} (b) (1.4-3.0) eq. CN^{-} and (c) emission spectra.

Sensitivity and Detection Limit for CN^-: For detections limit 7 sample of **2a+Co^{2+}** complex (5 μM) was prepared and plot a linear calibration curve which corresponding to change in emission intensities. The estimated standard deviation was found to be 132.84. The calibration sensitivity (m = 3222.748) for CN^- was predictable from the slope of the fluorescence curve obtained between change in fluorescence intensities ($F-F_0$) versus CN^- concentration. The F and F_0 indicate the emission intensities of **2a+Co^{2+}** complex in the presence and absence of CN^-, respectively. Limit of detection (LOD) estimated using equation LOD = 3σ/m. Where, *σ* illustrates standard deviation for blank solution of **2a+Co^{2+}** and *m* calibration sensitivity for CN^-.

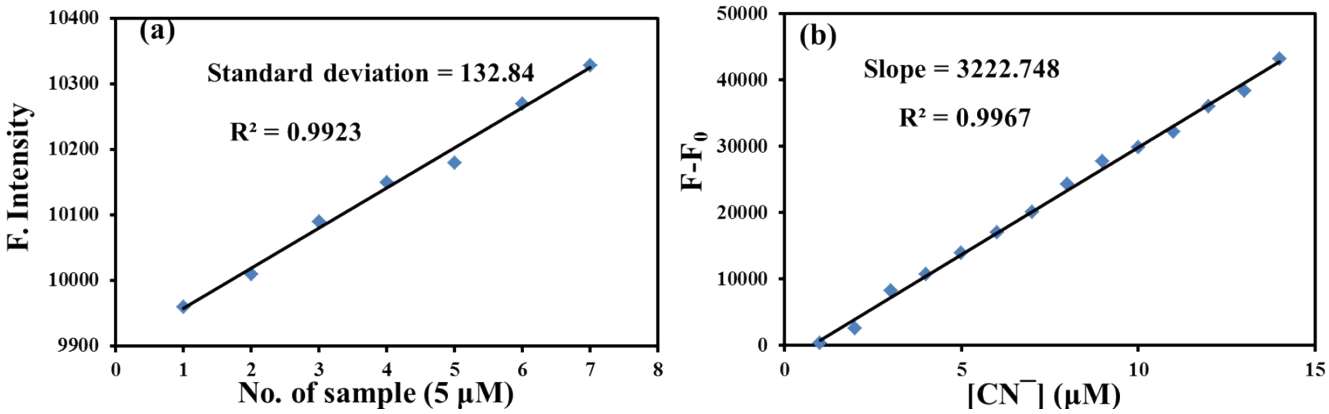

ESI Fig. S5: (a) Calibration curve for **2a+Co^{2+} complex** and (b) calibration sensitivity for **CN^-** ion in H_2O-DMF (1:9, v/v, HEPES buffer 7.4).

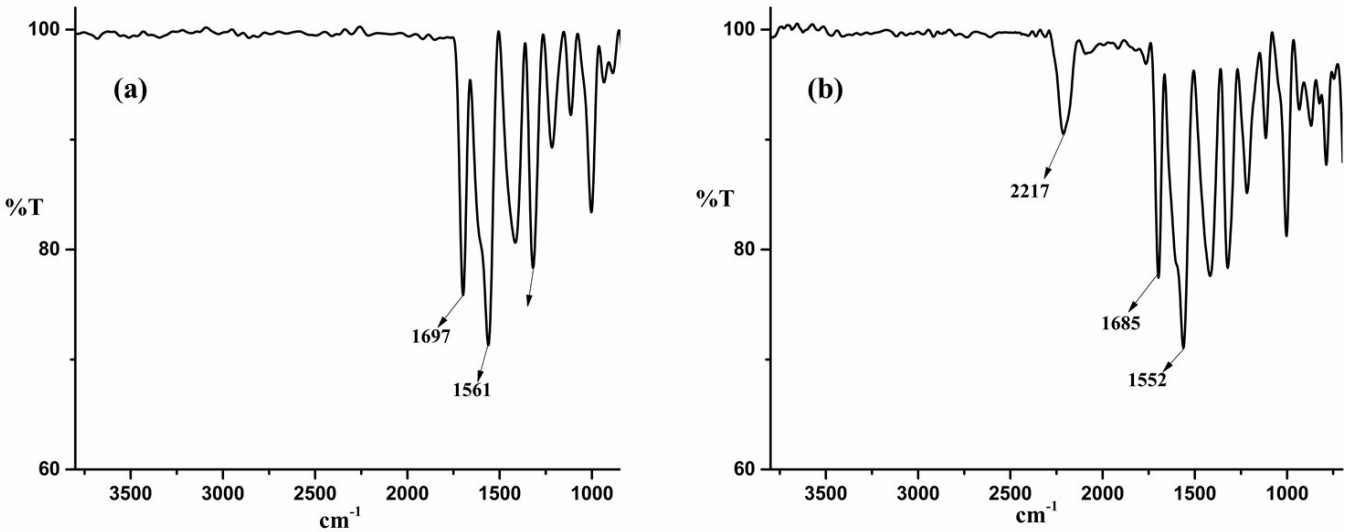

ESI Fig. S6: IR spectra of (a) **2a+Co^{2+}** complex and (b) **2a +Co^{2+}+CN^-** complex.

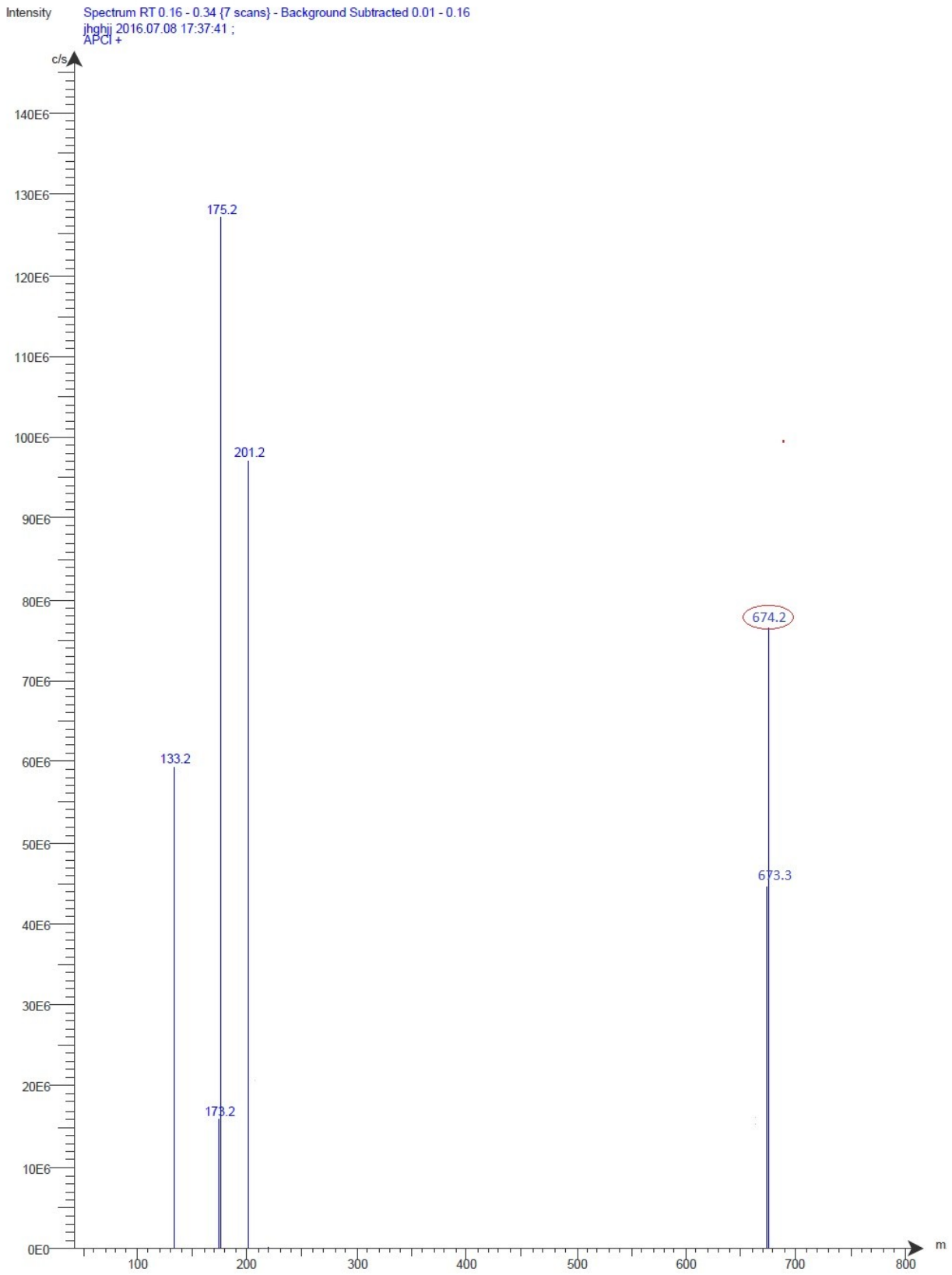

ESI Fig. S7: Mass spectrum of **2a+Co^{2+}** complex.

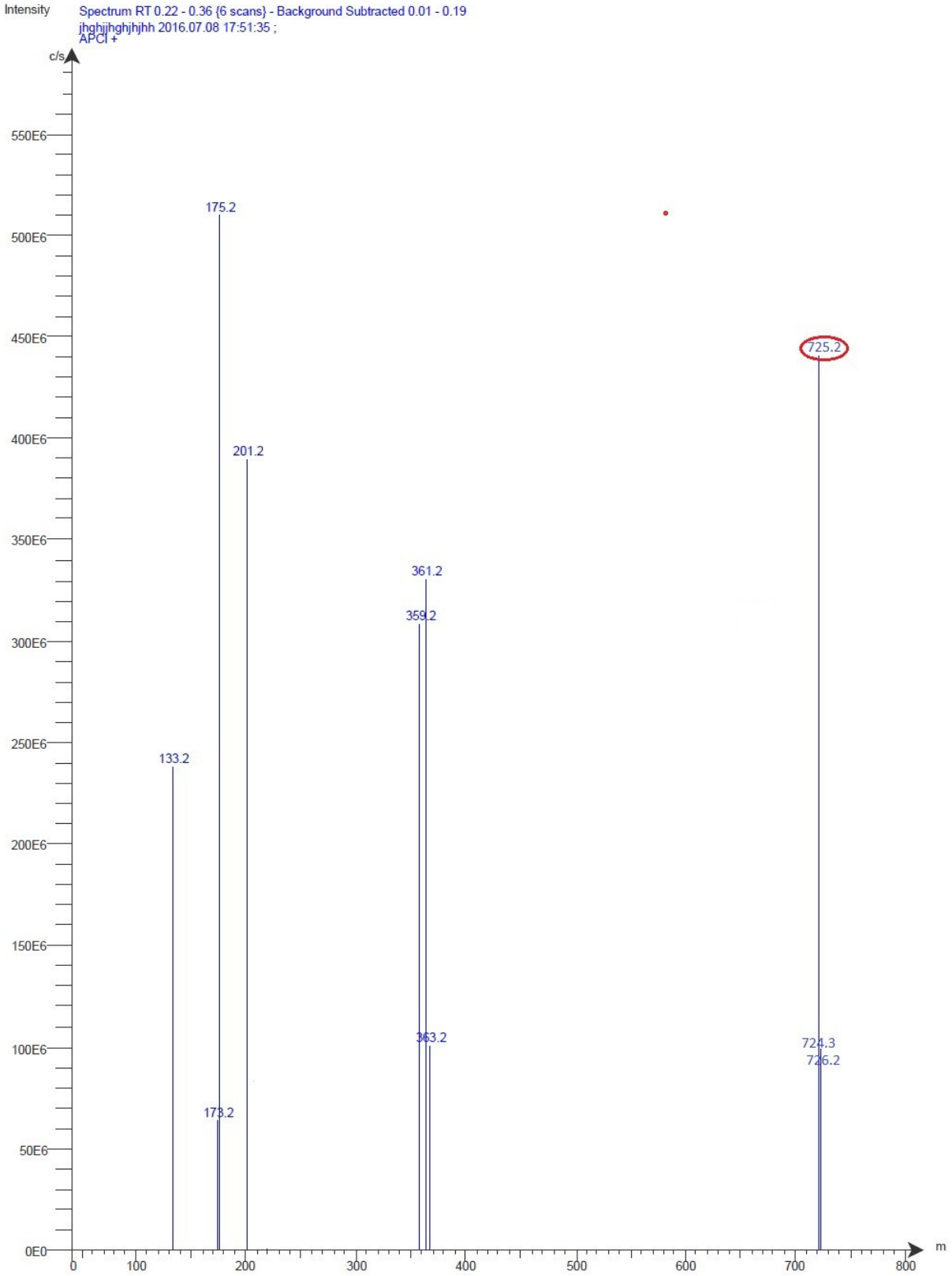

ESI Fig. S8: Mass spectrum of **2a** $+Co^{2+}+CN^{-}$ adduct.

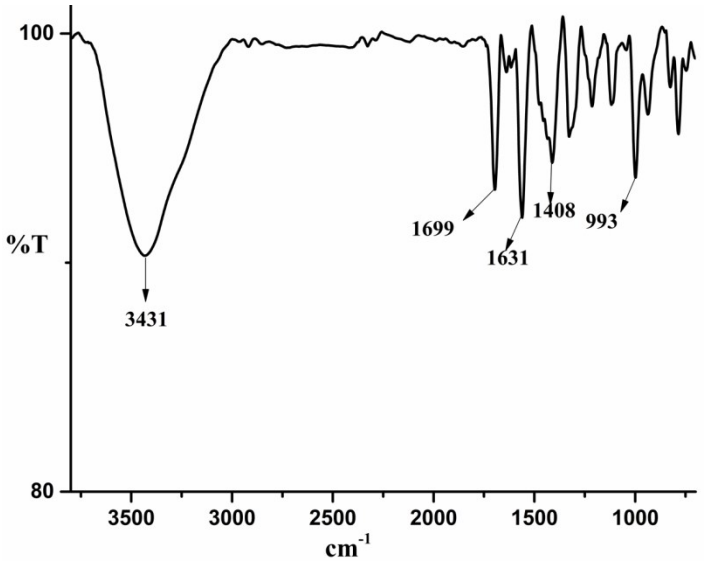

ESI Fig. S9: FTIR spectrum of **2a**.

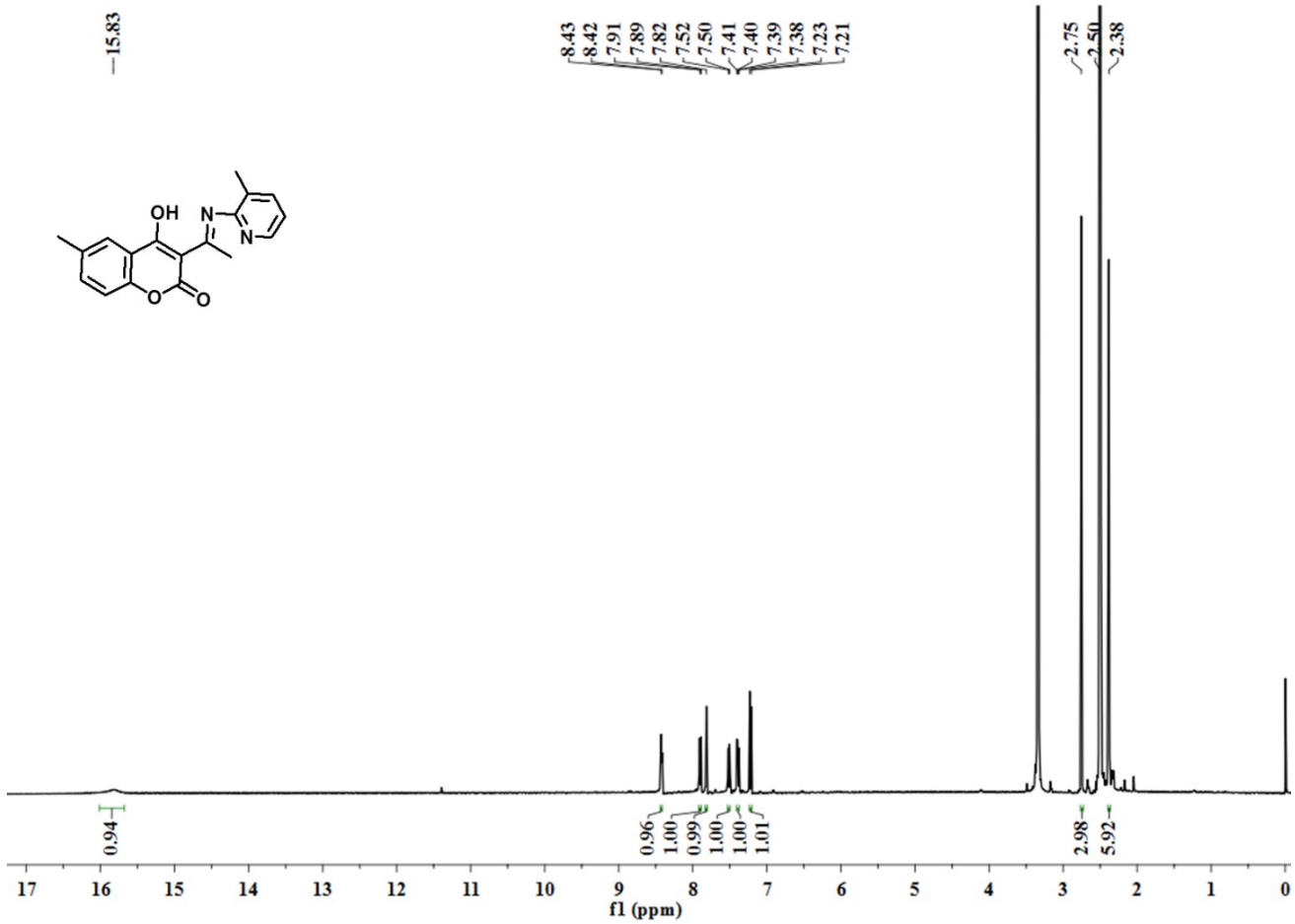

ESI Fig. S10: ^{1}H NMR spectrum of **2a** in d_6 DMSO.

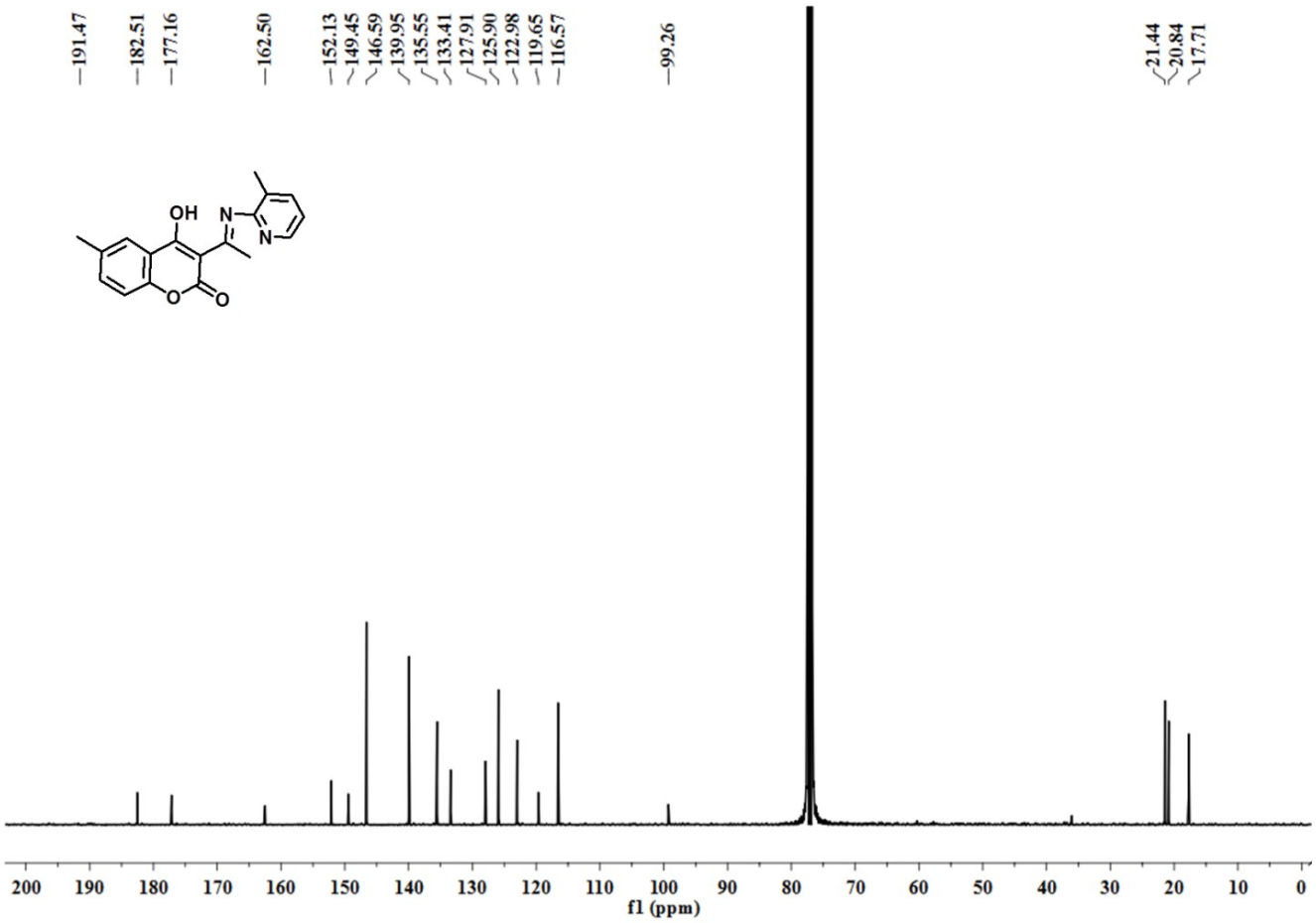

ESI Fig. S11: ^{13}C spectrum of **2a** in $CDCl_3$

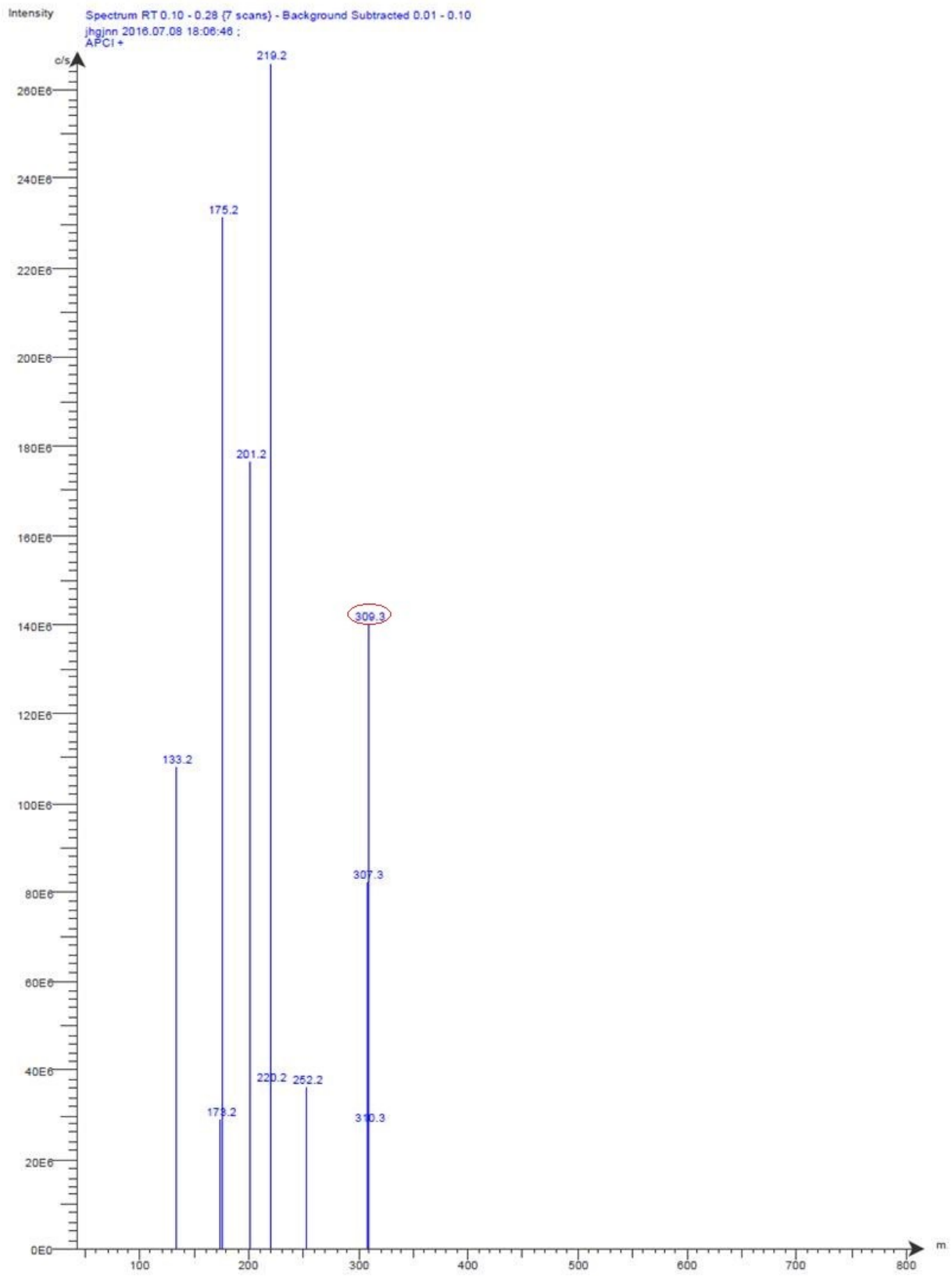

ESI Fig. S12: Mass spectrum of **2a.**

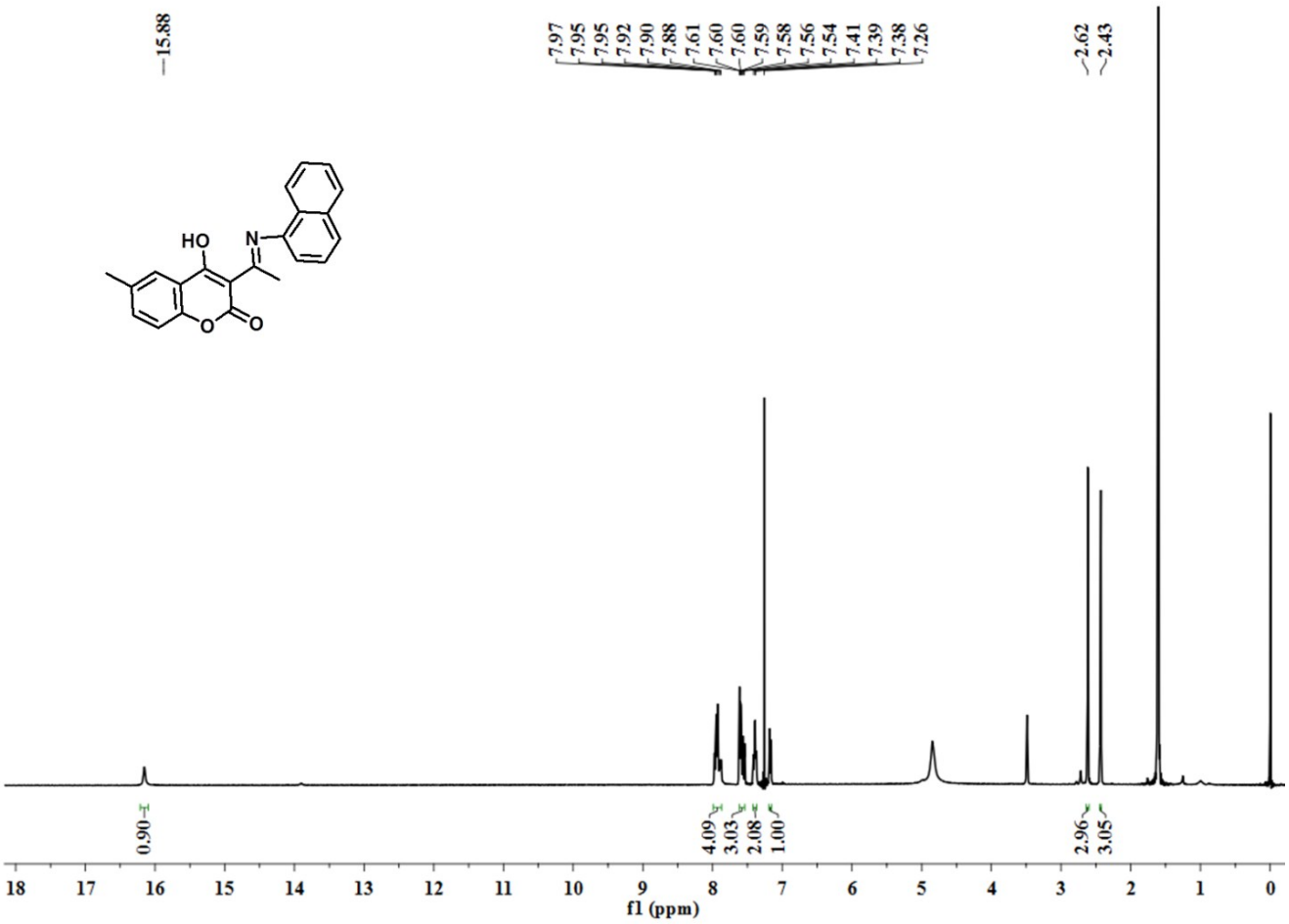

ESI Fig. S13: ^{1}H NMR spectrum of **2b** in $CDCl_3$

^{1}H NMR ($CDCl_3$-400MHz) δ/ppm: 15.88 (-OH, s 1H), 7.88-7.97 (m 4H, J-36), 7.54-7.61 (m 3H J-28), 7.38-7.41 (t 2H J-12), 7.26 (s 1H), 2.62 (s 3H), 2.43 (s 3H).

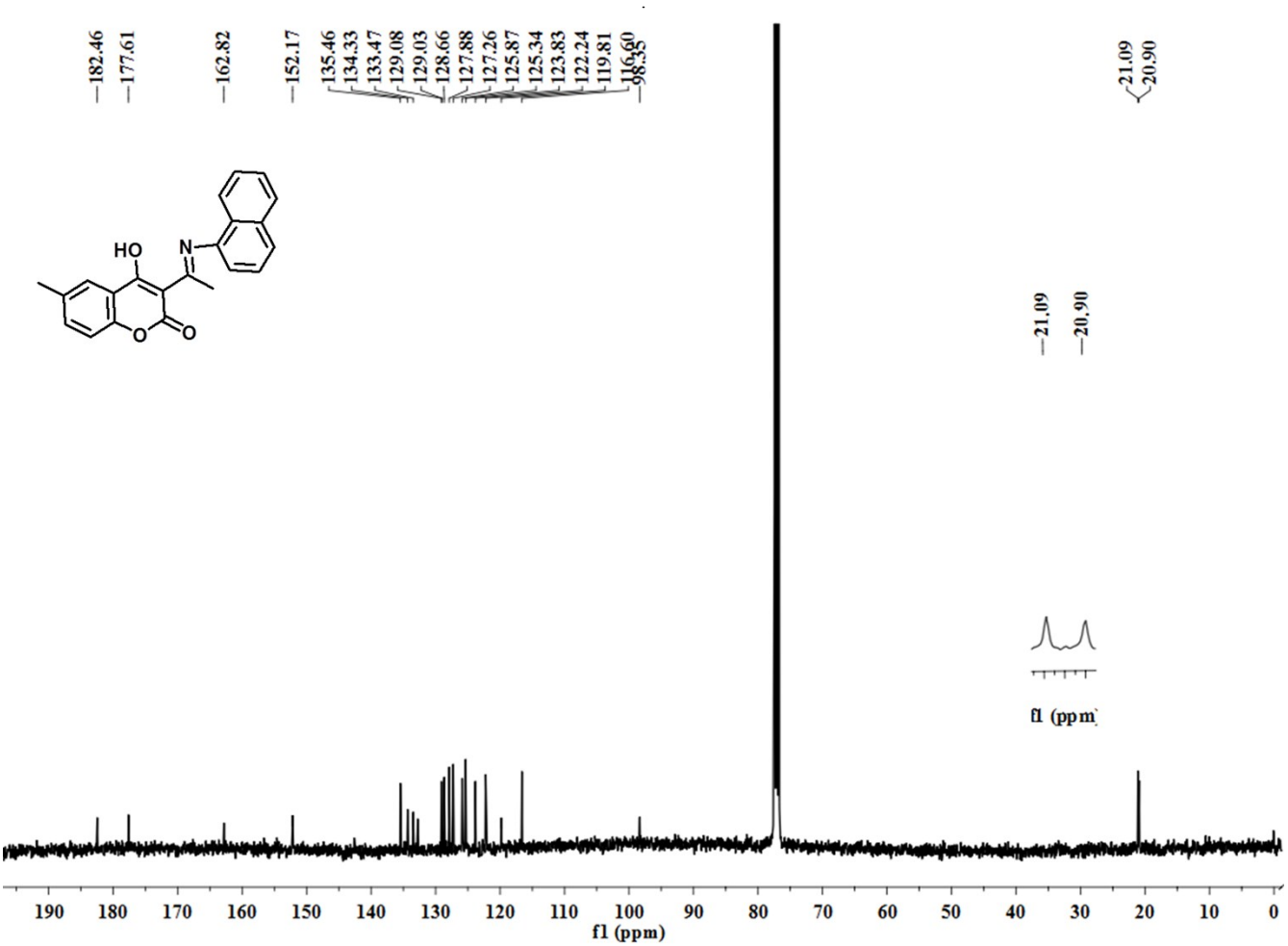

ESI Fig. S14: ^{13}C spectrum of **2b** in $CDCl_3$.

^{13}C NMR ($CDCl_3$ -100MHz) δ/ppm: 182.5, 177.6, 162.8, 152.2, 135.5, 134.3, 133.5, 132.8, 129.0, 129.0, 128.7, 127.9, 127.3, 125.9, 125.3, 123.8, 122.2, 119.8, 116.6, 98.4, 21.1, 20.9.

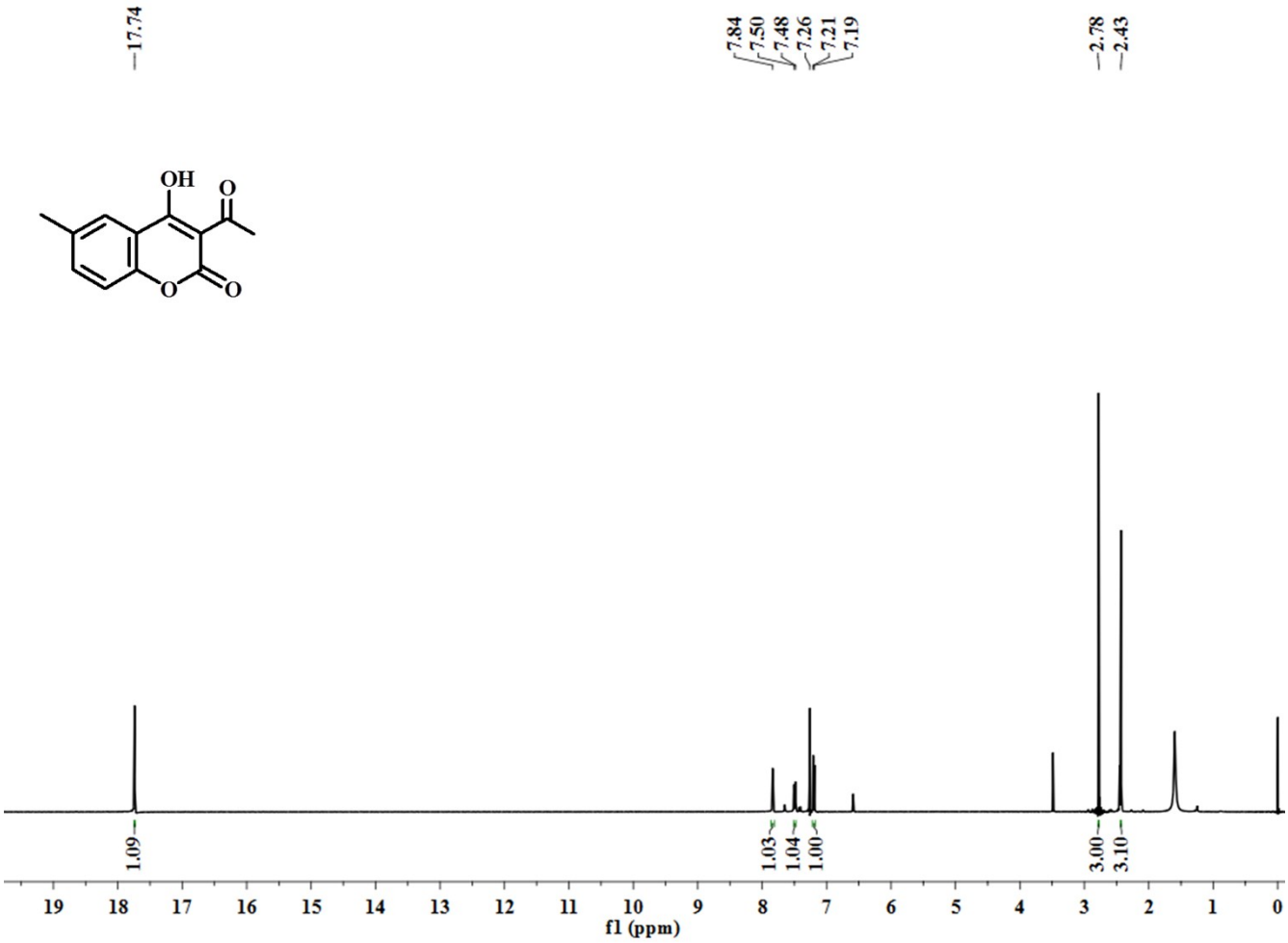

ESI Fig. S15: ^{1}H NMR spectrum of **1** in $CDCl_3$.

^{1}H NMR ($CDCl_3$-400MHz) δ/ppm: 17.74 (-OH, s 1H) 7.84 (s 1H), 7.48-7.50 (d 1H J-8), 7.19-7.21 (d 1H J-8), 2.78 (s 3H), 2.43 (s 3H).

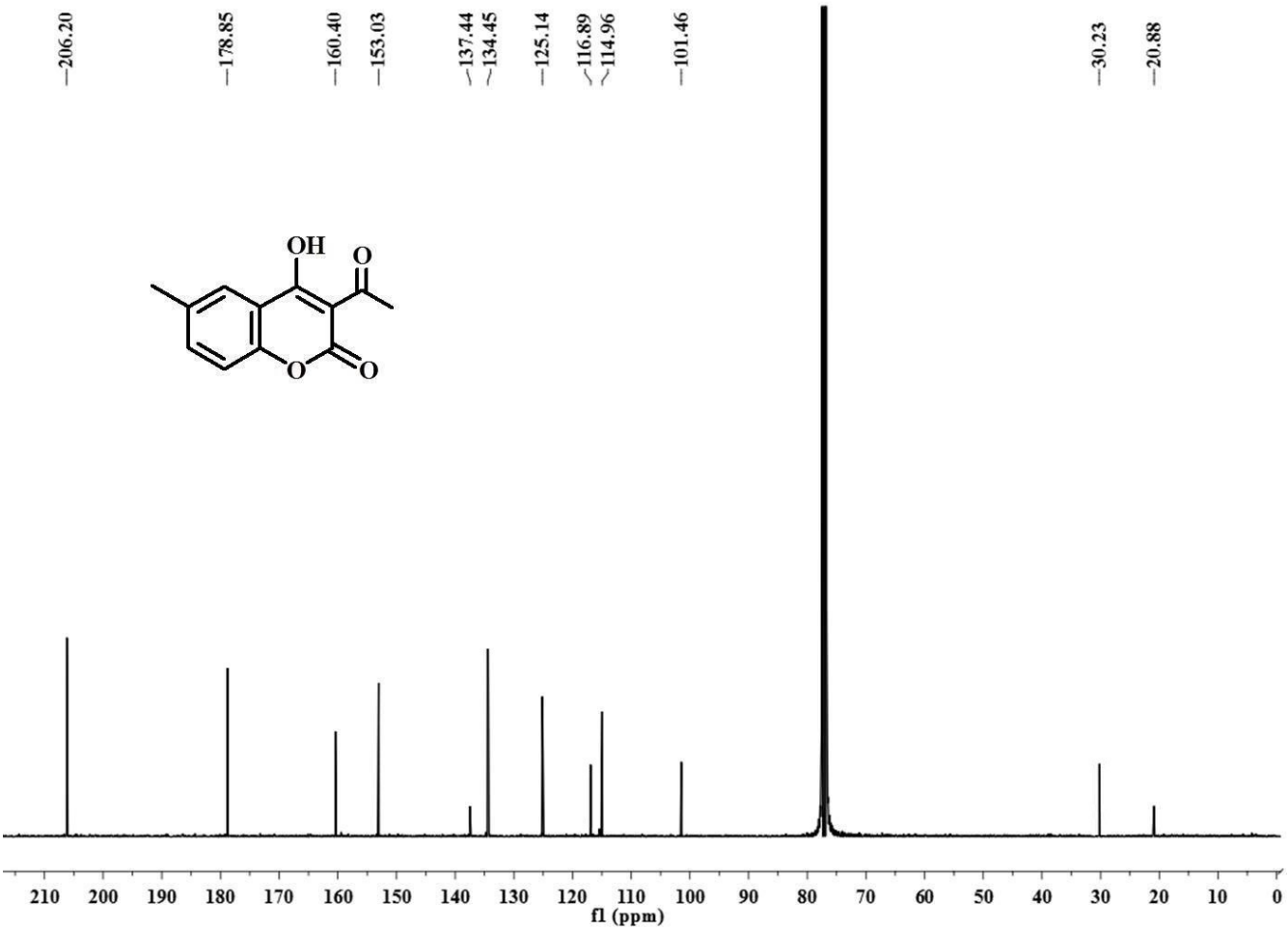

ESI Fig. S16: ^{13}C spectrum of **1** in $CDCl_3$.

^{13}C NMR ($CDCl_3$ -100MHz) δ/ppm: 206.2, 178.9, 160.4, 153.0, 137.4, 134.5, 125.1, 116.9, 114.9, 101.5, 30.2, 20.9.

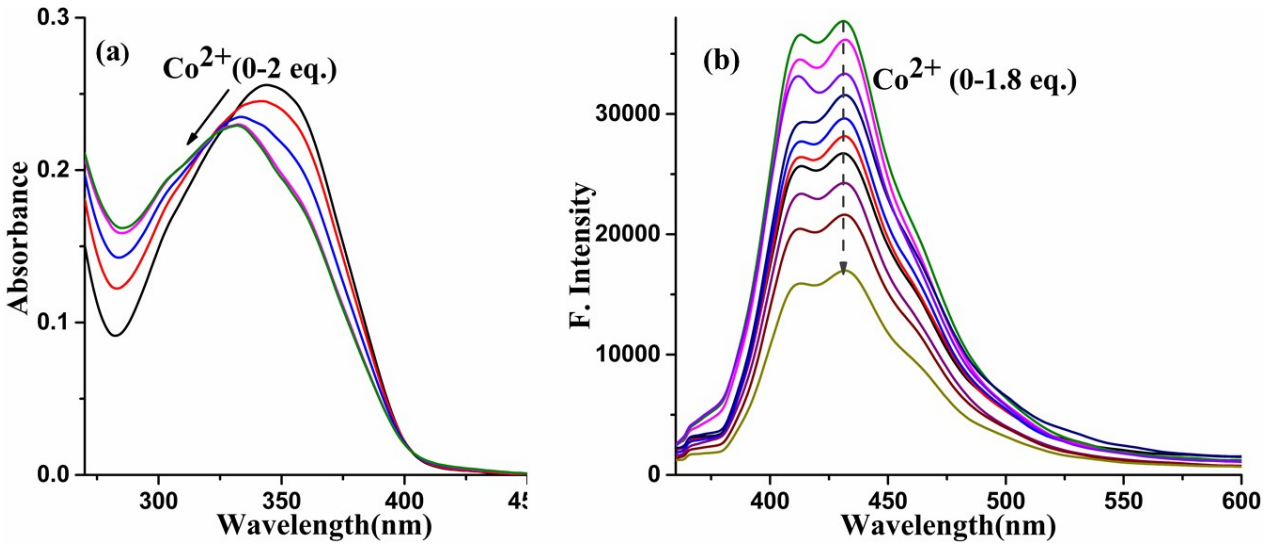

ESI Fig. S17: (a) Absorption titration spectra (b) Emission titration spectra of upon addition of Co^{2+} H_2O-DMF (1:9, v/v, HEPES buffer 7.4).

Table S1: Recovery analysis of spiked CN^- concentration in deionized water, river water and tap water samples[a].

Spiked Concentration(μM)	Deionized water		River water		Tap water	
	Found (μM)	Recovery (%)	Found (μM)	Recovery (%)	Found (μM)	Recovery (%)
0.00	0.01		0.06		0.02	
10	10.00	100 ± 1.2	10.16	101.6 ± 2.4	10.05	100.5 ± 3.8
20	19.98	99.9 ± 2.1	20.26	101.3 ± 3.1	20.08	100.4 ± 1.9

[a]Mean value ± standard deviation (triplicate measurements)